The Smell Engine: A system for artificial odor synthesis in virtual environments

Alireza Bahremand* Mason Manetta† Jessica Lai‡ Byron Lahey§ Christy Spackman¶
Brian H. Smith‖ Richard C. Gerkin** Robert LiKamWa††

Arizona State University

ABSTRACT

Mimicking physical odor sensations virtually can present users with a real-time odor synthesis that approximates what users would smell in a virtual environment, e.g., as they walk around in virtual reality. To this end, we devise a Smell Engine that includes: (i) a Smell Composer framework that allows developers to configure odor sources in virtual space, (ii) a Smell Mixer that dynamically estimates the odor mix that the user would smell, based on diffusion models and relative odor source distances, and (iii) a Smell Controller that coordinates an olfactometer to physically present an approximation of the odor mix to the user's mask from a set of odorants channeled through controllable flow valves. Through a three-part user study, we found that the Smell Engine can help measure a subject's olfactory detection threshold and improve their ability to precisely localize odors in the virtual environment, as compared to existing trigger-based solutions.

Index Terms: Human-centered computing—Interactive systems and tools; Computer systems organization—Sensors and actuators

1 INTRODUCTION

As humans, our sense of smell – also known as olfaction – allows us to navigate rich environments of scents that signal appetite, threat, nostalgia, and other feelings. Through mental association with previous experiences, olfaction allows us to prepare for the situation at hand. Infused alongside visual, auditory, and tactile cues, the spatial and temporal nature of odor allows humans to associate scents with specific objects and areas, thereby informing how to interpret and handle various situations, especially when navigating unfamiliar environments or events. Allowing virtual environments to similarly produce odors produce spatiotemporal olfactory cues would provide a platform for multisensory training, education, memory, and several other use cases. This is important for virtual reality and augmented reality, as immersive visual and auditory systems would be expanded with olfactory systems to accompany them.

As such, we see a compelling opportunity to synthesize physical odors that mimic what a user would experience while exploring an odor-infused virtual environment with virtual objects. While existing works can produce specific pre-mixed odor mixes and perfumes, as triggered by virtual cues, we aspire to design a virtual olfaction system that is more naturally integrated into spatiotemporal virtual environments among other multisensory stimuli. In particular, we look to design a software framework that is:

- *spatiotemporally reactive*, responsive to a user's position in relation to the odors and events in the virtual environment, modifying the mix and strength of the odors as they arrive at the user's virtual nose;
- *expressive in scent programmability*, offering developers and designers the ability to program a wide range of odor profiles, odor intensities, and odor dispersion characteristics into the virtual environment;
- *modular in operation*, providing hardware abstraction layers to control odor-synthesizing hardware and platform interfaces to explore further modes of odor-mixing hardware; and
- *multi-sensory in integration*, embedded in standard game engine design/development for integration alongside visual and auditory sensations.

Figure 1: The Smell Engine enables programmable scent-filled environments, consisting of scenes and objects with associated odors that render through an olfactory display.

To this end, we devise a Smell Engine that includes: (*i*) a Smell Composer framework that allows developers to configure odor sources in virtual space, (*ii*) a Smell Mixer that dynamically estimates the odor mix that the user would smell, based on diffusion models and relative odor source distances, and (*iii*) a Smell Controller that coordinates a hardware olfactometer to physically present an approximation of the odor mix to the user's mask from a set of odorants channeled through controllable flow valves. We implement and integrate our Smell Engine with the Unity Game Engine, allowing designers to place odors and specify their dispersion characteristics at design time, and stimulating distance-based odor mixing at runtime, produced through the hardware valve system. Our Smell Engine framework operates alongside existing visual and auditory systems of the Unity Game Engine, using the position of the user's virtual camera as a rough estimation of the position of the user's virtual "nose". Altogether, this provides an end-to-end system for artificial odor synthesis of virtual environments.

We evaluate our Smell Engine through measurement-based studies and user studies. We measure our system's odor generation precision by using a photoionization detector (PID) to measure outflowing gas concentration. We found that the Smell Engine can

*e-mail: abahrema@asu.edu
†email: mmanetta@asu.edu
‡email: jlai23@asu.edu
§email: Byron.Lahey@asu.edu
¶email: christy.spackman@asu.edu
‖email: brian.h.smith@asu.edu
**email: rgerkin@asu.edu
††email: likamwa@asu.edu

2642-5254/22/$31.00 ©2022 IEEE
DOI 10.1109/VR51125.2022.00043

produce granular changes in odor strength in scales ranging from 10.0 picomolar to 1.0 millimolar. [1]

For the user studies, we determine the system's timeliness of odor delivery, the system's ability to help identify a user's olfactory detection thresholds, and the system's ability to help improve user localization of odor sources in a virtual environment. With the first user study, we measure the user-perceived latency. We found that some users perceived odors relatively quickly, within 2.5 seconds, while others perceived odors more slowly, e.g., around 10 seconds. In our second user study, we used the Smell Engine to identify user-perceivable just-noticeable-difference (JND) thresholds for changes in olfactory stimulus magnitude. Not only could the Smell Engine help identify a subject's odor acuity levels, but it could generate odor concentrations at an even finer granularity than user-perceivable detection thresholds. For the final user study, we investigated how accurately users can localize an odor source between our approach for odor delivery and the traditional collider-based delivery method. The results show that our odor delivery method improved the average user accuracy of the group by 43% and improved the average proximity of their odor source localization by 55%.

In summary, we contribute a software-hardware framework that integrates olfactory stimuli into virtual environments, such that odor strengths spatiotemporally vary based on user navigation and interaction, presenting odors through a mask-based apparatus.

2 Related Work

Works in the human-computer interaction community have advanced the design and development of olfactory display technologies and virtualization of olfactory spaces. These describe common challenges, such as: *i)* supporting a large dynamic range of odor strengths (which is essential to perception because psychometric curves span many orders of magnitude), *ii)* providing fine temporal control for odor generation, *iii)* virtualizing the olfactory space in a scalable fashion. In this section, we outline the key advancements, capabilities, and limitations of these research spaces.

2.1 Olfactory Displays (Wearable and Desktop)

Olfactory display systems deliver olfactory stimuli through a variety of approaches, including Surface Acoustic Wave (SAW) devices [8], Piezoelectric sensors [2, 8, 19, 24, 25], ink-jet printers [20], and multi-component devices [6, 13–16]. In [11, 27], a desktop olfactory display system directs odorous airflow to physically collide and spatially disperse odorant molecules (OM) at the user's nose. Simplified inexpensive systems can also direct odorant airflow to a user by vaporizing a liquid odorant using a fan, microcontroller, and 3D printed enclosure [9]. Similarly, OSpace [6] presents scent-delivery with parametric adjustments in timing, relative intensity of constituent odorants, flow rates, and air extraction.

Other wearable olfactory display research, [7, 8, 17, 24, 26], investigates form factors of eyeglasses, necklaces, and VR HMD clamps, shortening the length/travel-time when delivering scents to the user's nose. In commercial realms, OVR Technologies - built a wearable olfactory display that attaches to VR HMDs, comprising swappable odor vials, a custom Unity API to assign scent parameters to objects, and a fan to clear out millisecond-long bursts of scented liquids. Although the system generates odors with different intensities, it is coarsely triggered by collider and reliant upon pre-mixed scent profiles rather than leveraging the chemical or physical properties of the odorants.

2.2 Virtually Parameterizing Olfactory Stimuli

To date, two approaches primarily account for how odor concentration varies spatially and temporally for a virtual environment: user-navigable collider-based systems [4, 8, 19] and Computational Fluid Dynamics (CFD) to calculate the airflow field and how an odor disperses [10, 12, 13]. These works demonstrate a tradeoff between computation time, wearability/portability, and accuracy of odor field virtualization.

Exploring the odor mixing capabilities of olfactory displays, [15] found that a modular system consisting of a micro-pump, liquid odorants connected to solenoid valves, and a SAW atomizer, can blend odors that are identical to pre-blended odors in liquid phase.To scale up the quantity of odorants and perceivable strength, [18] devised a 24-scent multi-sensory display capable of harnessing scent type, scent intensity, wind speed, and air temperature.

In favor of wearability and reduced computation time, [13] implemented a wearable olfactory display that atomizes a liquid odorant when the user virtually triggers a collider in the virtual environment. Similarly, Season Traveler [19] implemented a wearable olfactory that modulated piezo-electric sensors to vaporize a set of liquid odorants towards the user's nose upon virtual collision with an odor-trigger object. While innovative, the systems were confined to a limited set of achievable odor selections and strengths.

To explore accuracy in odor virtualization, [26] showed that an odor display can simulate a laminar-air flow model of user-perceived strength of an odor field by tuning parametric adjustments of delivery timing. Further improving accuracy in representing a virtual odor field, CFD simulations can model how odorant concentrations evolve in both space and time [10, 12]. In [13], a CFD solver generates a matrix-like lookup table for instant lookup of odor concentration strengths based on the airflow and dispersal of a particular odorant at a distinct location, e.g., user's location at any given point in time. Although this system model presents smells accurately, it suffers from intensivee computation time due to pre-calculation – iterating over every object and its position in virtual space – resulting in a fixed, static representation of the virtual odor space.

2.3 Multisensory VR Systems

To date, several studies have focused on multi-sensory system design, sensory substitution, and stereo-olfactory displays [4, 5, 18, 19, 23] Studying the impact and challenges of integrating and creating multisensory stimuli for VR experiences, [19] added olfactory and tactile (thermal and wind) stimuli to audio-visual stimuli. They found that users felt increased immersion with multiple perceptual stimuli; however, users were not able to strictly attribute presence and immersion to olfactory stimuli potentially because of the 'fundamental attribution error' [22]. This work raises the question of how critical it is that olfactory stimuli in virtual environments precisely replicate olfactory stimuli in real life for users to perceive the stimuli as 'real'. Novel research directions become available if stimuli experienced in virtual worlds can be mixed and used to reflect other stimuli sensations. For example, [4] developed a device that tricks users into perceiving thermal sensations by stimulating the users' trigeminal nerve, providing a better understanding of the relationships between thermal and olfactory stimuli.

To provide a sense of directionality for artificial olfaction, recent studies [5, 18] have explored stereo rendering of olfaction using chemical and electrical stimulation. In [3], a VR headset is equipped with a system that allows for switching between scents, altering the temperature of the air carrying the scents, changing the burst frequency of the scents, and specifying the directional airflow of the scents to the user using tubes clamped to the sides of the headset. In [5], Jas. et al create a stereo-smell experience via electrical stimulation by stimulating the user's trigeminal nerve through a device worn across a user's nasal septum. Mixing sensory stimuli in VR can push multisensory research in new directions.

[1] A molar unit represents the moles of solute per liter of solution.

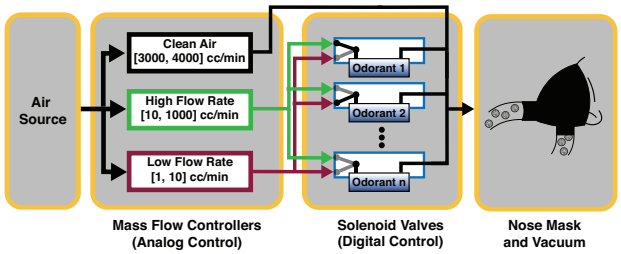

Figure 2: The Smell Engine has several independently controlled solenoid valves, each of which directs airflow derived from the air source across a single OM source with a high/low flow rate. Coming out of the olfactometer, the odorous air is merged with clean air and directed into the user's nose. A vacuum continuously clears out the air passage.

3 ODOR SCIENCE

3.1 Odor Mix Vector

Our perception of smell comes from specialized olfactory sensory neurons. Microscopic odorous molecules (OM)[2] bind to and activate specialized receptors on these neurons, which send messages to our brain, which decodes the activation of specific combinations of olfactory neurons into distinct smells. Most real odor mixtures – as experienced in nature – comprise different OMs at varying concentrations. Increasing the concentration of a single OM influences its perceived olfactory intensity, i.e. how strong it smells. Changing the relative concentration of OMs in a mixture can change the olfactory character of the stimulus, i.e., what is smells like.

For an odor to be detectable by a human, the concentration of at least one OM must exceed a detection threshold; for a change in concentration to be detected, the absolute change must exceed the so-called just-noticeable-difference (JND, also called "difference threshold" or δ_C), defined as the absolute difference in concentration required for detection of change from the initial concentration. Weber's Law (defined for all stimulus modalities, not just olfaction), states that the JND is a constant proportion of the original stimulus magnitude, i.e., that the ratio $k = \frac{\delta_C}{C}$ is a constant. A primary goal of the Smell Engine is to be able to produce odors at an appropriate resolution across the perceivable concentration range of OMs – high enough to replicate the smallest detectable changes in concentration.

To allow for controlled changes in perceived odor intensity, our system digitally parameterizes the physical properties of the OMs that are stored in the liquid phase in identical vessels. Parameters include vapor pressure, liquid-phase density, and molecular weight. From these values, our system computes the partial pressure of the vapor phase for each OM at steady-state within an associated vessel. Mixing these OMs produces an N-dimensional "Odor Mix" Vector, where N is the number of unique odorants in the virtual space.

3.2 Odor Delivery System (Olfactometer)

The odor delivery system is a dynamic dilution olfactometer: a consistent airflow source that mixes OMs by combining the independents vapors from one or more vessels attached to a manifold. The olfactometer operates with a fixed set of odorants distributed across a number of sealed vessels, capable of producing many combinations of odor mixtures. The specific odorants and concentration in each vessel must be determined in advance, but linear combinations can be delivered during the operation phase.

The olfactometer directs clean airflow through the headspace of vessels containing liquid odorants in an odorless solvent (light mineral oil). This is achieved using a manifold of programmable, digital solenoid valves and analog programmable mass flow controllers to provide precise flow rate through each vessel headspace, thus creating the OM composition of the resulting mixture. 10 L/min is a standard output flow rate for an olfactometer, formed from the combined output of the OM manifold and a clean air stream to achieve proper dilution. Solenoid valves direct the output of each vessel pneumatically to one of three paths: high flow (A), low flow (B), or no flow (Figure 2). Each valve is programmed such that each odor "frame" can contain any combination of state occupancy times that sum to the length of the frame (here, 1 second). This forms a duty cycle of active and inactive OM contribution.

The system uses Mass Flow Controllers (MFC) to govern the low flow and high flow paths, recomputed in each frame within each MFC's operating range. Each MFC is chosen to provide precise flow rate control in a different concentration regime (A: 1-1000 mL/min; B: 0.01-10 mL/min; Final: 0.01-10 L/min), and by combining them a high dynamic range is achieved. We aim to hold the total flow rate constant to produce a consistent user experience with constant air pressure. Total control over the composition of the Odor Vector – the time-varying concentration of each OM – is thus achieved by continuously and jointly setting the duty cycles of each solenoid valve and the flow rate setpoints of each MFC.

The odorous air output from the olfactometer is combined with clean air, then fed into a nose mask that nests/clamps over the user's nose, as illustrated in Figure 2. Attached to the bottom outlet of the nose mask is a vacuum that sucks odorous air from the nose mask every other 500 ms. If no odorous air is outputted from the olfactometer, then the user is continuously fed clean air. Altogether, our system directs constant airflow with partial flow rates over valve devices adjusted by a set of MFCs, recombined and fed into a nose mask worn on the user's nose.

4 SYSTEM DESIGN/METHODOLOGY

We design the Smell Engine to provide olfactory stimuli that are: i) spatially varying, ii) diverse and granular in user-perceivable strength, and iii) contextual to the virtual environment. To this end, the Smell Engine uses three primary components – as illustrated in Figure 3: a Smell Composer for design of virtual odor spaces, a Smell Controller for runtime computation of virtual odor mixes, and a Valve Driver to control hardware to produce physical odor mixes.

4.1 Designer Tools for Odor-Infused Environments

To allow designers to create a virtual scent-filled environment consisting of odorous objects and regions, we provide a **Smell Composer** framework that designers can use to specify Odor Source instances and locations. Designers do this by attaching *Odor Source* components to virtual objects, describing odor identity and propagation characteristics as attributes of the Odor Source. Odor Sources can also be attached to the entire virtual space, creating an "ambient smell" to the environment. The game engine can also modify Odor Source attributes at runtime, e.g., changing the odor strength over time, or swapping in different scents in response to a user button press. The designer can also modify Odor Source attributes at runtime, e.g., changing the odor strength over time or swapping in different scents in response to a user button press, via scripted events in the Unity Game Engine. Altogether, the Smell Composer framework provides a creative palette for designers to prepare virtual scenes imbued with odors.

The Odor Source interface allows the entry of the relative peak concentrations of odorant molecules (OM), creating the "scent profile" of the scent. Designers can also use the interface to specify the relative spread of each constituent OM, as shown in Figure 4, allowing the scent profile to change with distance. To identify OMs and reliably discern the chemical and physical properties of OMs as defined in Section 3.1, the Smell Composer interfaces with PubChem, an open chemistry database created by the National

[2]We use OM to refer to the molecule or to ensembles of the molecule.

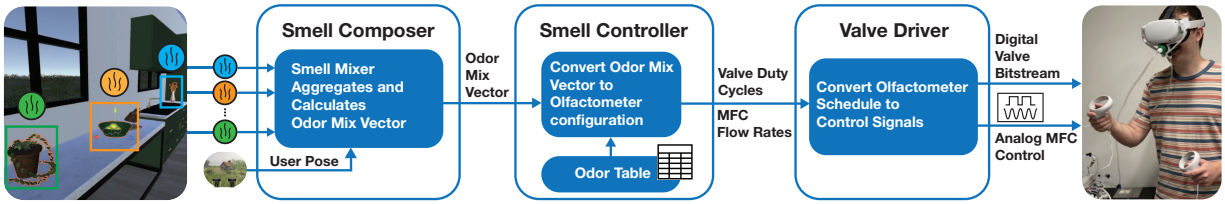

Figure 3: The Smell Engine consists of a Smell Composer, Smell Controller, and Valve Driver. Using the Smell Composer interface, designers create Odor Sources, which the Smell Mixer uses to calculate an Odor Mix Vector. The Odor Mix Vector is fed into the Smell Controller to determine an olfactometer hardware configuration. This configuration is then fed into the Valve Driver which actuates an olfactometer to generate the desired olfactory stimuli for the VR user.

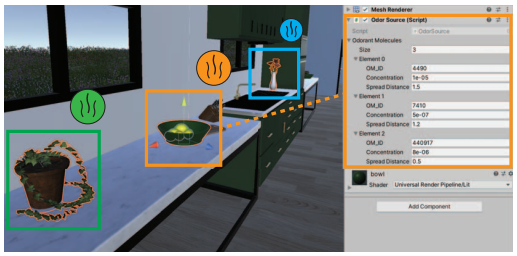

Figure 4: Using the Smell Composer's Odor Source interface, a designer can create an odor mixture by specifying constituent OMs, along with the OMs' relative peak concentration and relative spread.

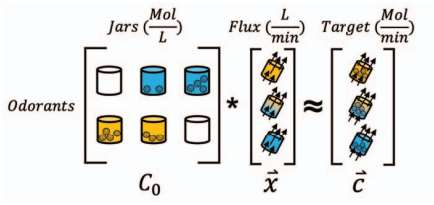

Figure 5: Using the set of available odorant concentrations C_0, the Smell Controller determines an optimal flux $\vec{x}$ in olfactometer scheduling that approximates the target Odor Mix Vector with an achievable Odor Mix Vector $\vec{c}$.

Institutes of Health. Using PubChem, the Smell Engine obtains each requested OMs vapor pressure, molar density, and molecular weight. Combined with the user-specified liquid volume of each OM per jar, the Smell Engine then determines each jar's vapor concentration by calculating the partial pressure and molarity of each present OM. By integrating PubChem's vast library of virtually identifiable OMs with the Odor Source interface, Smell Engine equips designers to create and modify virtual odor recipes using a wide range of olfactory specifications.

The Odor Source's spread distance and max concentration parameters allow a designer to specify diffusion properties of the odor, i.e., when and how much of the odor strength is to diffuse. Analogous to virtual audio stimuli in a Game Engine, changing the max concentration and spread of an Odor Source component is similar to changing the volume and spread of an Audio Source component. To elongate or shorten the gradual change of odor strength, designers adjust the spread distance parameter. If one constituent odorant of an Odor Source's set of odorants is more dominant in intensity over others, designers can modify the max concentrations to reflect this. By adjusting these parameters, designers can choreograph olfactory stimuli in virtual experiences such that odor strength becomes adaptive to user proximity. Using such a composition of odors, the scent of a lemon bowl, for example, will get stronger as a user approaches the fruit.

Following the audio stimuli analogy, Odor Sources function similarly to Audio Sources in that they can be dynamically positioned within the virtual environment, anchored to specific areas/regions, and assigned to game objects. Should the designer want an environmental smell for the virtual space with no associated game object/model, they can create an Odor Source instance fixed to the camera. If the designer wants an odor source to travel through the virtual environment, e.g., an NPC with an associated odor, they can assign an Odor Source instance to the moving game object.

4.2 Runtime for Mixing Odor Recipes at the Virtual Nose

With Odor Sources defined and instantiated at design time, the goal of the Smell Engine at runtime is to aggregate all Odor Sources into a single Odor Mix Vector at the user's virtual nose, which then is used to faithfully match the virtual odor composition with a physical odor composition. Similar to audio stimuli in a game engine, a **Smell Mixer** can be thought of as an Audio Listener; the Smell Mixer receives input from all stimuli sources, then renders the aggregate stimulus for the user to trigger hardware actuation.

To determine the Odor Mix Vector relative to a user's position, the Smell Mixer uses an atmospheric diffusion equation defined by [21] to spatially present odors in a virtual environment. Through this equation, we emulate the aggregation of spatially-varying concentration profiles of the N molecular odorants, which are indexed by $i \in \{1,N\}$, as they present themselves through M virtual odor sources, indexed by $j \in \{1,M\}$. As the user moves farther from the odor source, modeled by their distance x_j from the odor source, the concentration profile diminishes through atmospheric diffusion along a Gaussian relationship with odorant-specific σ_i dispersion coefficients. Based on such modeling, the odor synthesis system aggregates perceived concentration of each odorant as a sum across all odor sources: $m_i = \sum_j c_{i,j} e^{x_j^2/\sigma_i^2}$. Together, these concentrations form a Odor Mix Vector m of target odorant concentrations. With this Odor Mix Vector, scents of various programmable objects can naturally compete and combine before artificial synthesis.

4.3 Controller to synthesize physical OM recipe from virtual odor mix vector

The Smell Mixer transmits its calculated Odor Mix Vector to the **Smell Controller**, a subsystem process for configuring an olfactometer on-the-fly to delivering dynamically mixed odors. Given the Odor Mix Vector, the Smell Controller specifies a scheduled duty cycle of valve states to control odorant exposure times and Mass Flow Controller (MFC) flow rates to regulate the airflow volume through the valves. To determine when and how much of an odorant must be diffused through the system's airflow, the Smell Controller calculates the amount of flux needed to achieve a target concentration using a set of variables that are representative of the system's physical components. As shown in Figure 5, we define C_0 as the matrix representing the available set of

odorant concentrations in each jar, $\vec{x}$ as the flux, and $\vec{c}$ as the target concentration. To represent flow rates and valve duty cycles, we define f_A as the flow rate of MFC A, f_B as the flow rate of MFC B, i as the index of a jar, and n as the number of jars. We use w_{iA} and w_{iB} as the occupancy time in ms of valve i in state A and state B, respectively. The flux y_i going through a jar i can thus be calculated using the following equation:

$$y_i = f_A \frac{w_{iA}}{\sum_{k=1}^{n} w_{kA}} + f_B \frac{w_{iB}}{\sum_{k=1}^{n} w_{kB}} \quad (1)$$

As discussed in Section 3.2, the hardware capabilities of the olfactometer's components have various constraints that manifest as parameter constraints in our optimization function to approximate the flux. For example, for our specific olfactometer hardware configuration, we use the following set of constraints: $0.01\frac{cc}{min} \leq fB \leq 10\frac{cc}{min}$; fA + fB $\leq 1000\frac{cc}{min}$; 0 s $\leq w_{iA} \leq 1s$; $0s \leq w_{iB} \leq 1s$w$_{iB} = 0s$, if $w_{iA} > 0s$; $w_{iA} = 0s$, if $w_{iB} > 0s$

Because the airflow is divided amongst all active jars, creating the denominator terms in Equation 1, the optimization is too computationally intensive to resolve at runtime. Thus, we use an odor table to precompute solutions for a different flow rate and duty cycle combinations within the available constraints. The odor table contains 48 concentration setpoints evenly spaced on a logarithmic scale ranging from [1 nanomolar, 1 micromolar], eight MFC flow rate setpoints spanning across three orders of magnitude [0.1 cc/m to 1000 cc/m], and 18 valve occupancy times, evenly spaced on logarithmic scale, occupying up to 1 second. Organized as a KD-Tree, the odor table determines which combinations of olfactometer flow rates and duty cycles over the OM odorants in the jars that generate the achievable Odor Mix Vector that approximates the target Odor Mix Vector from the Smell Mixer, as shown in Figure 5.

4.4 Olfactometer hardware control for odor synthesis

Given the Smell Controller's scheduled valve duty cycles and MFC flow rates, the **Valve Driver** executes the schedule using multifunction I/O modules provided by National Instruments. Illustrated in Figure 3, the Smell Controller's schedule is converted into digital and analog control signals that are used by the system to direct the odorants' vaporized air-flow through a series of tubes that are connected to the solenoid valves and MFCs, diffused into a nose mask, and sucked through using a continuously running vacuum.

The Valve Driver interfaces through the NIDAQmx API to issue multiplexed digital and analog signals that correspond to scheduled valve states and MFC flow rates. The Valve Driver issues valve duty cycles as 32-bit digital values; the first 16 bits represent high states, the lower 16 bits representing low states; zeros represent off states, while ones represent on states. The Valve Driver formats and converts issued MFC flow rates as a list of analog voltage values.

5 Evaluation Setup

We conducted system tests and user studies to evaluate the effectiveness of the Smell Engine in delivering olfactory stimuli of varying odor strengths. For the system tests, we use a photo-ionization detector (PID) to evaluate the precision in which the Smell Engine synthesizes odorants at desired concentrations. Our user studies aim to evaluate how well our system can help determine a subject's odor sensitivity levels and how our approach improves their ability to navigate virtual worlds using olfactory cues. For the user studies, we recruited a total of 15 subjects (11 male, 4 female) to participate in the three-part study, contingent on their ability to perceive all odors presented. Through the user studies, we identify: 1) the user-perceived latency for odor delivery; 2) how coarsely or finely users can identify different odorant strengths; and 3) how effectively users can localize virtual odor sources. No user subject reported any history of a medical condition that reduced their sense of smell. The study was approved by the university's IRB and the subjects were recruited from within the university via email posting.

5.1 Odorant/Scent Selection

For our system tests, we used ethanol because it provides a strong and consistent PID response, and the kinematics (e.g., vapor pressure) of ethanol are similar to our selection of odorants. Our odorant selection for user studies consisted of Acetophenone, Carvone, and D-limonene, as safe, readily accessible odorants. Generally, users reported that Acetophenone smelt sweet like berries, Carvone smelt like peppermint, and D-limonene smelt like oranges.

Each odorant was prepared manually at different dilutions – 10:1 for Acetophenone, 1:1 for Carvone, and 10:1 for D-limonene – using light, odorless mineral oil as the solvent. We loaded these odorants into glass jars attached by PTFE tubing to an aluminum manifold.

6 Odor Synthesis Precision

Using a PID to monitor and measure the gas concentration, we evaluate the precision with which the Smell Engine synthesizes odor concentrations. With the PID sensor readings, we compare the ratio changes in voltage against the ratio changes in specified concentrations to determine the precision of our system. To validate system/hardware controllability for odor synthesis, we measured PID response when changing duty cycles of the solenoid valves and airflow rate setpoints of the Mass Flow Controllers. To evaluate the precision, we compare the ratio difference in PID sensor readings between starting and target concentrations by increasing the concentration values at a granular level.

6.1 Trial Procedure

Our experimental setup consists of a push-to-connect pneumatic fitting that connects the odorous air, a vacuum, and the PID septum into the sealed-off outlet. To ensure reliable PID readings for each trial we: 1) measure clean air at steady-state as a reference point, 2) wait for PID response to achieve steady-state for each target concentration or hardware configuration, and 3) measure clean air again to account for sensor drift. Using this testing process, we conduct a series of experiments to vary the valve duty cycles and MFC flow rates to evaluate the relationship from the PID response.

In the first experiment, we evaluate the relationship between the PID response and valve duty cycle by gradually increasing the relative valve occupancy time from 0 to 1000 ms in 100 ms increments. In each trial, we increase the flow rate setpoint by a fourth of its max capacity (i.e., [2.5 cc, 5.0 cc, 7.5 cc, 10.0 cc] for MFC B and [250 cc, 500 cc, 750 cc, 1000 cc] for MFC A). The carrier MFC supplements the remaining airflow needed to meet the constant flow rate target. In the second experiment, to understand the relationship between MFC setpoints and PID response, we conducted a series of tests, incrementally increasing the MFC setpoint with different duty cycle configurations. For the last experiment, we evaluate the precision of odor synthesis for six trials. In this experiment, we test 16 different concentrations, ranging from 1 picomolar to 1 micromolar.

6.2 Results

Shown in Figure 6, our results illustrate a relatively linear relationship between PID sensor readings and increased valve occupancy times or increased MFC flow rates. Illustrated with the subplots in Figure 6, we observe that lower flow rates achieve a high-precision range of 10.0 mV, whereas higher flow rates achieve a coarse range of 3 V. The ratio difference for PID sensor readings in a high versus a low state is consistent with the ratio difference of airflow between MFC A and MFC B, an approximate 3 order of magnitude difference. With the occupancy subplots in Figure 6, we observe an approximate 1:4 ratio for a quarter usage of an MFCs

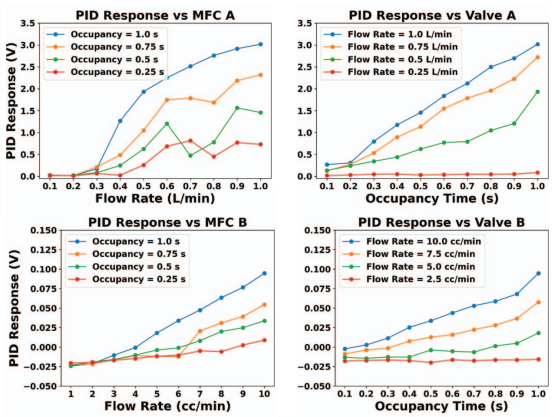

Figure 6: PID sensor readings for increased valve occupancy times and MFC flow rates. We adjust MFC A flow rate (top left), MFC B flow rate (bottom left), relative valve occupancy time in a high flow rate state (top right), and in a low flow rate state (bottom right).

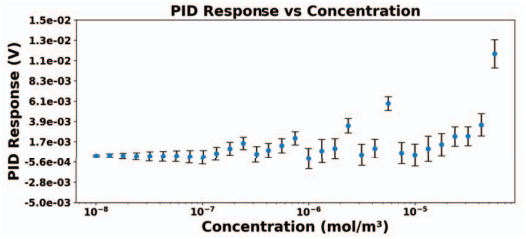

Figure 7: PID sensor readings across 6 trials for entire concentration range, demonstrating increasing variation with larger concentrations.

max flow rate compared to the max flow rate of the MFCs. Similarly, for the flow rate subplots in Figure 6, we observe an approximate 1:4 ratio for a quarter valve duty cycle compared to the max valve duty cycle. As seen with all data points in the subplots, the combination of increased MFC flow rates and valve duty cycles results in a higher PID response, presenting a monotonically increasing relationship.

Figure 7 illustrates the PID sensor readings for target concentrations comprising varied valve duty cycles and MFC flow rates. From this data, we observe a roughly increasing PID response with higher concentrations. The observed plateau in PID response is in accordance with the previous system tests, validating a roughly linear relationship within the picomolar range.

7 User Study 1: User-Perceived Latency

In this section, we evaluate the user-perceived latency of the Smell Engine's odor diffusion capabilities. For this experiment, we diffuse each odorant at its max concentration, i.e., max flow rate and valve duty cycle. In addition to measuring the user-perceived odor diffusion latency, we use this experiment as a screening session to determine whether a subject can smell the odorants. If a subject does not have sensitivity to the odorants, then we do not proceed with the rest of the study. This excluded 5 out of the 15 participants.

7.1 Trial Procedure

For this study, users trigger a clicker to activate olfactory stimuli and trigger it again when olfactory stimuli are perceived. This experiment is repeated three times for each odorant, generating three latency measurements for each odorant. If the subject cannot perceive the stimuli within 15 seconds for 2 out of 3 trials for any odorant, we conclude that the subject cannot perceive the stimuli.

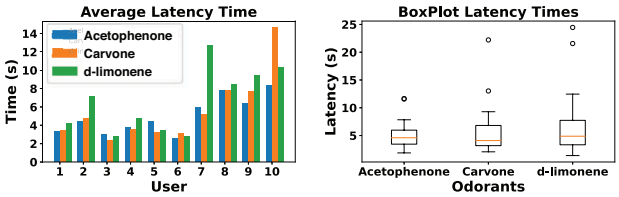

Figure 8: User-perceived latency for each odorant. Subjects that could not perceive the odor are shown as anomalies.

7.2 Results

We find that our users perceived the system-generated odors from 2.5 to 10 seconds after the virtual triggering of the odor, (with two outliers at 12 and 14 seconds). The variation seemed to be user-specific, i.e., some users perceived odors faster than other users. Among our users, the average user-perceived latency of our system's odor diffusion capabilities is approximately 5.7 seconds. Despite having a small sample size, we conducted an ANOVA for multiple comparisons and found that the influence of odor type on user-perceived latency was not statistically significant ($p > 0.05$). With Figure 8, we observe that some users perceive smells faster than others. Additionally, we observe that 75% of the user subjects perceived all diffused instances of the odorants within a 10-second time frame, depicted in Figure 8. For this study, four subjects could not perceive at least one of the odorants within the threshold timeframe; for these subjects, we did not move forward with the rest of the study. In a future study, we would like to collect additional demographic info and test more familiar and less familiar smells.

8 User Study 2: Just-Noticeable-Difference Odorant Concentration Strengths

In this study, we aim to understand how effectively our system can help determine user-sensitivty levels for specific odors by measuring the user-reported just-noticeable-difference (JND) values for the olfactory stimuli. As described in Section 3.1, a JND value quantifies the amount by which a change in stimulus intensity produces a noticeable variation in the human sensory experience. This information is invaluable as it helps us better understand the relationship between olfactory stimulus intensity and user perception.If our system can generate odor concentrations that are more granular than the average user perceivable JND values, we could devise a screening system to determine a subject's odor acuity level. Such a capability would be especially useful in modeling subject perception of olfactory stimulus over time.

Realizing these opportunities, we investigate user-reported minimum odor strengths for each odorant and JND concentration values relative to different baseline concentrations: 0 molar, 10 picomolar, 100 nanomolar. For the second baseline, we start with 10 picomolar because of the limited achievable concentration strengths of the odorants. For this first study, we hypothesize that a user using our system can identify a subject's JND odorant concentration value relative to the starting concentration value.

8.1 Trial Procedure

To discover JND concentration values, we implemented a staircase procedure to identify each user's perceptual threshold. The staircase procedure is an iterative process that, given a starting stimulus strength X, will increase/decrease the intensity of the stimulus X by a delta, y, until a subject specifies a perceived change in stimulus strength. After the subject perceives the change in stimulus strength three times, we average the recorded $X+y$ threshold values. The result is a user-specific JND value such that $X \pm y$ is not differentiable from X if $y < JND$ and is differentiable from X if $y > JND$. We conducted this study with ten subjects, none of whom reported any former medical issues that would influence their sense of olfaction.

For each trial in this study, we present the subject with the baseline concentration X, along with the increased odor concentration Y, in a randomized order. We then prompt the participant to confirm whether they noticed a difference in odorant concentration strength. At the start of each odor concentration, the subject places the nose mask and is able to sniff for up to 10 seconds. After concentrations X and Y are presented to the participant, we prompt them to confirm whether they noticed a difference in odorant strength. If a user subject reports no difference in odor strength, Y continues to increase by a concentration value, h, which is a multiple of the baseline. Should the user subject report a difference in odor strength, we halve h and decrease Y by h to determine a more granular *JND* value. Once a subject reports a difference three times, we average the Y concentrations and record the result as the subject's *JND* value.

For the first trial, the baseline is no concentration strength ($X = 0$) and the starting concentration is 10 picomolar ($Y = 10^{-11}$). For the second trial, the baseline is 50 nanomolar ($X = 5 \cdot 10^{-8}$) and the starting concentration is 60 nanomolar ($Y = 6 \cdot 10^{-8}$). For the third trial, the baseline is 10 picomolar ($X = 10^{-11}$) and the starting concentration is approximately 13 picomolar ($Y = 1.316^{-11}$). This procedure is repeated for all odorants.

8.2 Results

In support of our hypothesis, the results suggest that the Smell Engine can help identify a subject's JND relative to the starting odorant strength. The box-and-whiskers plots in Figure 9 visualize the variance in JND results for the different baseline concentrations. From this data, we found that participants were less sensitive to changes in strength for D-limonene compared to the other odorants, suggesting that the Smell Engine can be used to identify how perceivable an odor is for individual users or groups of users. Figure 9 illustrates how subject JND values changed across trials. Because some subjects did not perceive a change in strength three times, there may be no connection between some baseline trials.

Consistent with the Weber-Fechner Law, we observe that the level at which users perceive a change in stimulus intensity is proportional to the initial stimulus intensity. For example, the general distribution of user-reported JND values for the clean air baseline is more sensitive than at the 10.0 picomolar baseline trial. Figure 9 shows that user-reported JND values are small when starting with a lower baseline concentration (e.g., 0, 10^{-11}) and large when starting with a higher baseline concentration (e.g., 5×10^{-8}). Generally, we found that the average JND value for all odorants is within two orders of magnitude relative to the baseline. In a future study, we will investigate user-reported JND values with more baseline concentrations spanning multiple orders of magnitude.

Illustrated in Figure 9, we observe varying distributions of user-reported JND values for each odor and their respective baseline concentrations. The variation of user-reported JND values suggests that our system can produce perceivable odor concentrations that span multiple orders of magnitude. Additionally, these distributions demonstrate our system's ability to generate concentration strengths that are more granular than the JND values.

From Figure 9, which illustrates how subject JND values vary relative to the baseline, we found that several participants became more sensitive to granular changes in odor strength. For example, when comparing the 10.0 picomolar and clean air baseline trials, we see occasional instances where user-reported JND values became finer. This finding motivates the potential of improving a subject's ability to identify changes in odorant strength over time. In a future study, we will observe how exposure to specific odors over time influences a subject's sensitivity to the smell.

Interestingly, in some trials where the concentration baseline was large, subjects could not perceive changes in odorant strength despite noticing changes in stimulus strength for a lower baseline. Additionally, in some instances, subjects could not perceive a change in stimulus strength nor perceive the odorant itself, resulting in a significant variance of JND values. For example, with Carvone and D-limonene, the median is approximately 100 picomolar for test trials involving the picomolar and clean air baselines, suggesting that the outliers are pulling up the 75th percentile. For test trials that use the picomolar and clean air baselines, we found the distribution is larger than the trial that uses 50.0 nanomolar as the baseline.

9 User Study 3: Localizing Virtual Odor Sources

The goal of this study is to determine the extent to which our system improves a user's ability to localize odor sources in a virtual environment compared to existing trigger-based solutions. With this study, we measure subject accuracy in correct odor localization using two different odor delivery methods. For our approach, the dynamic odor delivery method, concentration is a function of distance, gradually getting more potent with user proximity. By contrast, with trigger-based odor delivery, the concentration is fixed and activated when the subject is within a 1.8 meter distance. Since in our pilot studies, most users would only start registering the dynamic delivery at 1.8 meter out, the 1.8 meter radius was set so that both the trigger and dynamic delivery methods would have the same radius of initial detection. For this study, we hypothesize that there is a difference in the probability of correctly localizing an odor source between the odor delivery methods previously described, such that the dynamic delivery method yields improved accuracy.

9.1 Trial Procedures

The experimental design for this study consists of two trials in which the subject is prompted to correctly identify all odor sources in the virtual environment within a five-minute time frame.

Both trials consisted of three rooms that each contained an odor source, as illustrated in Figure 10. We adopted a within-subject design in which odor delivery method and odorant type were the independent variable, and both accuracy and proximity of odor source selection were the dependent variables. To ensure participants relied on olfactory cues, we designed the VR environments to consist of similar layouts, primitive shapes/objects, a limited color palette, and the same odorants. Because this study is intended to study odor localization and not odor mixing, each room only contains one odor source. For each trial, we randomized the location of the odor source.

Subjects reported familiarity with VR and reported no past signs of olfactory-related diseases or surgeries. Before the study, the proctor helped the user put on the VR HMD, positioned the nose mask for comfort, and briefed them on the task. Subjects went through a tutorial scene that explained navigation and selection controls. Illustrated in Figure 10, the subjects navigate the virtual environment to select and specify odorous objects. Throughout the time of each trial, we recorded the subject's location, object interactions/selections, and final selections. The participants completed a motion sickness questionnaire before and after the study. Additionally, the participants completed a questionnaire evaluating the ease of identifying an odor source for each odor delivery method.

9.2 Results

Our main finding is that the dynamic-based odor delivery improved user accuracy in identifying virtual odor sources compared to the trigger-based approach. Using an ANOVA for multiple comparisons, we found that the influence of the odor delivery method on accuracy and proximal selection was statistically significant ($p < 0.05$).

Illustrated with Figure 10, we found a 43% average improvement in accurate odor localization with the dynamic delivery method. The average accuracy was 13.3% for the trigger-based odor delivery method, while the dynamic-based odor delivery method was 56.6%. With trigger-based odor delivery, only 2 of the ten participants were able to accurately localize an odor source. With dynamic delivery, all participants correctly localized at least one odor source precisely.

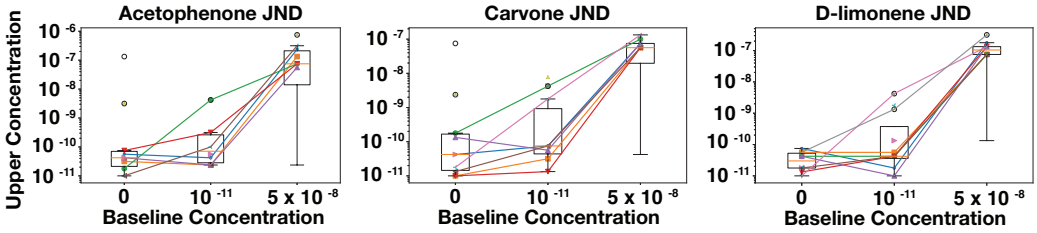

Figure 9: User-perceived JND results for different relative baselines. Each color represents one of the ten different users.

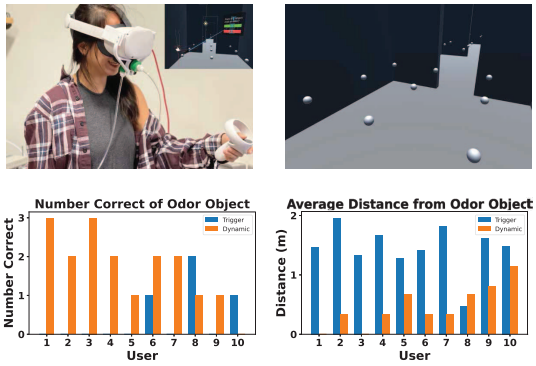

Figure 10: The subject navigates and sniffs around an environment that consists of 3 rooms with 9 spheres, one of which is an odor source (top row). For each user, we count the number of correctly identified odor sources and average distance to the odor source selection using two different odor delivery methods (bottom row).

From the charts in Figure 10, we found that participants were on average within 0.46 meters when attempting to localize the odor source with the dynamic-based delivery method. Using the trigger-based delivery method, participants were on average 1.45 meters off in odor source selection. With the detection threshold of 1.8 meters, we found that compared to the trigger-based odor delivery method, participants were on average 55% closer in proximity for odor source localization with dynamic-based odor delivery.

We found correlations between odor-specific JND values, latency measurements, and accuracy in odor localization with dynamic delivery. For example, only 20% of users accurately localized D-limonene, which was associated with the smallest distribution of JND values and the highest average detection latency. With Acetophenone and Carvone, which had a more diverse distribution of JND values, more than 70% of users accurately localized the smells. Our system can be used to study the ability to detect, identify, and localize different odors for different user populations.

When reviewing the post-study survey, we found that the rated ease for localization with the dynamic-based odor delivery method was higher than the trigger-based odor delivery method. Several participants remarked that it was easier to localize the odor source with the dynamic-based odor delivery method. No users reported signs of motion sickness after both trials of the VR experience.

10 Discussion

The results of our evaluation suggest that the Smell Engine can generate changes in odor strength that are more granular than user detection thresholds. Additionally, the Smell Engine can help identify a subject's odor sensitivity levels and improve their ability to localize odor sources within a virtual environment.

Our current system also has limitations. The physical tubing that connects the olfactometer to the user's nose restricts physical movement. Furthermore, the tubing system creates a multi-second latency due to the odor travel time, a known issue in the community for olfactometer-based olfactory displays [6, 8, 14, 22]. We also found that our system's nose mask does not comfortably support all nose shapes, causing us to omit one user study. We are investigating mask-based and mask-less wearable olfactory display designs that meet a wider range of profiles. We are also currently engaged in future work to evaluate our system's ability to mix odors on the fly.

We also envision that we can advance the project by: i) exploring an olfactory runtime for dynamic, on-the-fly odor mixing [1] using various forms of odor theory [28], ii) reducing latency in odor delivery by offloading on-device computation towards new wearable form factors, and iii) building a malleable software pipeline for odor diffusion to support various hardware designs (e.g., SAW atomizers, trigeminal peripherals). These could be facilitated through edge computing to accelerate software-hardware systems for real-time computation of physics-based modeling [13] that adaptively respond to dynamic scenes and user movements [4, 19, 24].

11 Conclusions and Future Work

A Smell Engine capable of computing and delivering olfactory cues on the fly in a virtual reality environment offers significant opportunities for a range of olfactory needs. These include opportunities for odor-oriented training and education, as well as basic scientific research, e.g., investigating whether humans identify and classify odors based on statistical co-occurrence of odorants, or more complex societal questions around cultures around smell. Virtual augmentation with dynamic, temporally and spatially delivered olfactory cues offers novel opportunities for examining, leveraging, and enhancing human olfaction.

To this end, we devise Smell Engine as a software-hardware framework that integrates olfactory stimuli into virtual environments such that the odor strengths are spatiotemporally varying based on user navigation and interaction. We evaluate the Smell Engine through measurement-based PID system studies and a three-part user study. From our set of PID tests, we found that the Smell Engine can generate coarse and granular changes in odor strength. The results of our user studies (N=10) suggest that the Smell Engine can help identify whether a user can perceive a specific odor and help determine what their detection threshold is for the specific odor. Additionally, we found that our system can improve a user's ability to localize artificially generated odor sources within a virtual environment, as compared to existing trigger-based solutions.

Acknowledgments

This research was supported by the NSF Next Generation Networks for Neuroscience Program (Award 2014217), the ASU Interplanetary Initiative, the ASU School of Life Sciences, the ASU School of Arts, Media and Engineering, the ASU School for the Future of Innovation in Society, the ASU Mayo Clinic Seed Grant, and National Institutes of Health (NIDCD R01DC017757 and R01DC018455, NINDS U19NS112953). Special thanks to Dylan Kerr for the design and build of the headset nose clamp.

REFERENCES

[1] A. Bahremand, C. Spackman, R. C. Gerkin, R. LiKamWa, and B. H. Smith. Virtually composing and dynamically mixing complex odors. In *Proceedings of the ACM CHI Smell, Taste, Temperature*, 2021.

[2] A. Batch, B. Patnaik, M. Akazue, and N. Elmqvist. Scents and sensibility: Evaluating information olfactation. CHI '20, p. 1–14, 2020. doi: 10.1145/3313831.3376733

[3] A. Batch, B. Patnaik, M. Akazue, and N. Elmqvist. Scents and sensibility: Evaluating information olfactation. In *Proceedings of the 2020 CHI Conference on Human Factors in Computing Systems*, CHI '20. Association for Computing Machinery, New York, NY, USA, 2020. doi: 10.1145/3313831.3376733

[4] J. Brooks, S. Nagels, and P. Lopes. Trigeminal-based temperature illusions. In *Proceedings of the 2020 CHI Conference on Human Factors in Computing Systems*, CHI '20, p. 1–12. Association for Computing Machinery, New York, NY, USA, 2020. doi: 10.1145/3313831.3376806

[5] J. Brooks, S.-Y. Teng, J. Wen, R. Nith, J. Nishida, and P. Lopes. Stereosmell via electrical trigeminal stimulation. CHI '21. Association for Computing Machinery, New York, NY, USA, 2021. doi: 10.1145/3411764.3445300

[6] D. Dmitrenko, E. Maggioni, and M. Obrist. Ospace: Towards a systematic exploration of olfactory interaction spaces. In *Proceedings of the 2017 ACM International Conference on Interactive Surfaces and Spaces*, ISS '17, p. 171–180. Association for Computing Machinery, New York, NY, USA, 2017. doi: 10.1145/3132272.3134121

[7] D. Dobbelstein, S. Herrdum, and E. Rukzio. Inscent: A wearable olfactory display as an amplification for mobile notifications. In *Proceedings of the 2017 ACM International Symposium on Wearable Computers*, ISWC '17, p. 130–137. Association for Computing Machinery, New York, NY, USA, 2017. doi: 10.1145/3123021.3123035

[8] K. Hashimoto and T. Nakamoto. Tiny olfactory display using surface acoustic wave device and micropumps for wearable applications. *IEEE Sensors Journal*, 16(12):4974–4980, 2016. doi: 10.1109/JSEN.2016.2550486

[9] M. Howell, N. Herrera, A. Moore, and R. McMahan. A reproducible olfactory display for exploring olfaction in immersive media experiences. *Multimedia Tools and Applications*, 75, 10 2016. doi: 10.1007/s11042-015-2971-0

[10] H. Ishida, H. Yoshida, and T. Nakamoto. Introducing computational fluid dynamics simulation into olfactory display. *Electrical Engineering in Japan*, 177(1):65–72, 2011. doi: 10.1002/eej.21087

[11] H. Matsukura, T. Yoneda, and H. Ishida. Smelling screen: Development and evaluation of an olfactory display system for presenting a virtual odor source. *IEEE transactions on visualization and computer graphics*, 19:606–15, 04 2013. doi: 10.1109/TVCG.2013.40

[12] H. Matsukura, H. Yoshida, H. Ishida, A. Saitoh, and T. Nakamoto. Odor presentation with a vivid sense of reality: Incorporating fluid dynamics simulation into olfactory display. In *Proceedings of the 2009 IEEE Virtual Reality Conference*, pp. 295–296, 2009. doi: 10.1109/VR.2009.4811062

[13] T. Nakamoto, T. Hirasawa, and Y. Hanyu. Virtual environment with smell using wearable olfactory display and computational fluid dynamics simulation. In *Proceedings of the 2020 IEEE Conference on Virtual Reality and 3D User Interfaces (VR)*, pp. 713–720, 2020. doi: 10.1109/VR46266.2020.00094

[14] T. Nakamoto, S. Ito, S. Kato, and G. P. Qi. Multicomponent olfactory display using solenoid valves and saw atomizer and its blending-capability evaluation. *IEEE Sensors Journal*, 18(13):5213–5218, 2018. doi: 10.1109/JSEN.2018.2834953

[15] T. Nakamoto, M. Kinoshita, K. Murakami, and A. Yossiri. Demonstration of improved olfactory display using rapidly-switching solenoid valves. In *Proceedings of the 2009 IEEE Virtual Reality Conference*, pp. 301–302, 2009. doi: 10.1109/VR.2009.4811065

[16] T. Nakamoto and H. P. D. Minh. Improvement of olfactory display using solenoid valves. In *Proceedings of the 2007 IEEE Virtual Reality Conference*, pp. 179–186, 2007. doi: 10.1109/VR.2007.352479

[17] OVR. https://ovrtechnology.com/. 2021.

[18] B. Patnaik, A. Batch, and N. Elmqvist. Information olfactation: Harnessing scent to convey data. *IEEE Transactions on Visualization and Computer Graphics*, 25(1):726–736, 2019. doi: 10.1109/TVCG.2018.2865237

[19] N. Ranasinghe, P. Jain, N. Thi Ngoc Tram, K. C. R. Koh, D. Tolley, S. Karwita, L. Lien-Ya, Y. Liangkun, K. Shamaiah, C. Eason Wai Tung, C. C. Yen, and E. Y.-L. Do. Season traveller: Multisensory narration for enhancing the virtual reality experience. In *Proceedings of the 2018 CHI Conference on Human Factors in Computing Systems*, p. 1–13. Association for Computing Machinery, New York, NY, USA, 2018. doi: 10.1145/3173574.3174151

[20] J. Sato, K. Ohtsu, Y. Bannai, and K.-i. Okada. Effective presentation technique of scent using small ejection quantities of odor. In *Proceedings of the IEEE Virtual Reality Conference*, pp. 151–158, 2009. doi: 10.1109/VR.2009.4811015

[21] K. Snitz, A. Yablonka, T. Weiss, I. Frumin, R. M. Khan, and N. Sobel. Predicting odor perceptual similarity from odor structure. *PLoS Comput Biol*, 9(9):e1003184, 2013.

[22] C. Spence, M. Obrist, C. Velasco, and N. Ranasinghe. Digitizing the chemical senses: Possibilities & pitfalls. *International Journal of Human-Computer Studies*, 107, 06 2017. doi: 10.1016/j.ijhcs.2017.06.003

[23] R. Trotta, D. Hajas, J. Camargo Molina, R. Cobden, E. Maggioni, and M. Obrist. Communicating cosmology with multisensory metaphorical experiences. *Journal of Science Communication*, 19, 04 2020. doi: 10.22323/2.19020801

[24] Y. Wang, J. Amores, and P. Maes. On-face olfactory interfaces. In *Proceedings of the 2020 CHI Conference on Human Factors in Computing Systems*, CHI '20, p. 1–9. Association for Computing Machinery, New York, NY, USA, 2020. doi: 10.1145/3313831.3376737

[25] B. Wu, Q.-H. Meng, H.-R. Hou, M. Zeng, and P.-F. Qi. An olfactory display system integrated with video content recognition. In *Proceedings of the 13th World Congress on Intelligent Control and Automation (WCICA)*, pp. 1641–1646, 2018. doi: 10.1109/WCICA.2018.8630614

[26] T. Yamada, S. Yokoyama, T. Tanikawa, K. Hirota, and M. Hirose. Wearable olfactory display: Using odor in outdoor environment. In *Proceedigns of the 2006 IEEE Virtual Reality Conference (VR 2006)*, pp. 199–206, 2006. doi: 10.1109/VR.2006.147

[27] Y. Yanagida, S. Kawato, H. Noma, N. Tetsutani, and A. Tomono. A nose-tracked, personal olfactory display. 01 2003. doi: 10.1145/965400.965481

[28] Y. Zhou, B. H. Smith, and T. O. Sharpee. Hyperbolic geometry of the olfactory space. *Science Advances*, 4(8), 2018. doi: 10.1126/sciadv.aaq1458